Amorphous carbon films for use as both variable-transmission apertures and attenuated phase-shift masks for DUV lithography

David L. Windt and Raymond A. Cirelli

Bell Laboratories, Lucent Technologies
Room 1D-456, 600 Mountain Ave.
Murray Hill, NJ 07974

Accepted for publication in J. Vac. Sci. Technol. B, March 1999

Amorphous carbon films for use as both variable-transmission apertures and attenuated phase-shift masks for DUV lithography

David L. Windt and Raymond A. Cirelli

Bell Laboratories, Lucent Technologies
Room 1D-456, 600 Mountain Ave.
Murray Hill, NJ 07974

windt@bell-labs.com
www.bell-labs.com/user/windt

Abstract

We describe the development of amorphous carbon (a-C) films grown by magnetron sputtering for use in optical elements for sub-0.25-micron DUV lithography. We have measured the transmittance of a-C films deposited onto quartz substrates as a function of film thickness, and find that the films are ideally suited for use in variable transmission apertures that can be used to improve DUV process latitude: we can achieve essentially any transmittance (T) desired in the range $0 < T < 100\%$ by controlling the film thickness (t) in the range $200 > t > 0$ nm with sub-nanometer precision. We also find that that the transmittance remains stable after prolonged exposure to high intensity DUV radiation. We describe a masked deposition technique to produce variable transmission apertures using a-C films of various thickness, and also discuss the use of these films in attenuated phase-shift masks, given that we can simultaneously achieve ~6-8% transmittance and a phase shift of 180° at either λ=248 nm or λ=193 nm.

1. Introduction

Recently we presented experimental results demonstrating a technique using a variable transmission aperture (VTA) for improving process latitude (i.e., depth of focus and resolution) in DUV (248 nm) lithography[1]. The VTA, consisting of a particular, two-dimensional spatial arrangement of amorphous carbon (a-C) films of various thickness (and thus various transmittance) deposited onto a quartz substrate, is placed between the source and the mask in a DUV stepper; and is used to control the distribution of light incident on the photo-mask, and thus the distribution of light diffracted from the features on the mask and reaching the wafer plane. The two-dimensional spatial transmission function of the VTA (i.e., as determined by the two-dimensional film thickness function) is designed for optimal process latitude for the feature geometry specific to a given photo-mask.

We describe here how these a-C films are produced with sub-nanometer thickness control using magnetron sputtering, and present measurements of transmittance as a function of film thickness at λ=248 nm. We also describe measurements of the film transmittance over time after prolonged exposure to high-intensity DUV radiation. These results are presented in Section 2, while in Section 3 we describe the masked deposition technique we have developed to produce the VTA's just discussed. We summarize our results in Section 4, and also discuss the use of these films in attenuated phase-shift masks, in light of the observation that we can simultaneously achieve ~6-8% transmittance and a phase shift of 180° at either λ=248 nm or λ=193 nm.

2. Film Preparation and Characterization

The films described here were grown by DC magnetron sputtering in argon of 99.999% purity, using a deposition system having sub-nanometer film thickness control for the production of multilayer X-ray optics that has been described previously [2]. The system is cryo-pumped (the background pressure was $5.0\pm0.1 \times 10^{-6}$ Torr) and the argon pressure was maintained at 1.5 mTorr with a closed-loop gas-flow system using a capacitance manometer and a mass-flow controller. The power to the 50-cm-long x 9-cm-wide planar magnetron source containing a solid graphite target (99.999% purity) was fixed at 400±7 W.

The deposition rate under the conditions just described was found to be 0.05 nm/s, and was computed from film thicknesses determined by X-ray reflectance analysis, described below. Film thicknesses were adjusted with sub-nanometer control by varying the (computer-controlled) rotational velocity of the substrate (which faces downward) as it travels over the source (which faces upward, 10 cm below the plane of the substrate.)

X-ray reflectance measurements are made as a function of grazing incidence angle at a fixed wavelength, using a four-circle diffractometer with a rotating anode X-ray source having a Cu target, and a pyrolytic graphite monochromator tuned to the Cu-Kα line near 8 keV (1.54 Å.) Reflectance measurements are typically made for incidence angles in the range 0° – 3°, which generally corresponds to a span of roughly 7 orders-of-magnitude in reflected intensity. The angular resolution of the diffractometer is ~0.02°, and measurements are typically made every 0.01°, sufficient to resolve the thickness fringes for films as thick as ~50 nm. Fits to the X-ray reflectance data, performed with the IMD software package [3], are used to determine film thickness and roughness. With this technique, the measured reflectance-vs.-incidence angle data is compared with a theoretical reflectance curve computed using an algorithm based on recursive application of the Fresnel equations; the formalism described by Stearns [4] is used to account for the effects of interfacial roughness (or diffuseness.) Non-linear, least-squares curve fitting (based on the X^2 test-of-fit) is used to determine the film thickness with a precision of approximately ±0.1 nm.

Films of various thickness in the range $2 < t < 100$ nm were deposited onto 15-cm-diameter x 0.5-mm-thick quartz substrates, and their normal-incidence transmission was measured using a Hewlett-Packard UV diode array spectrophotometer with collimating optics; the precision of the measurements is ± 3%. The resultant plot of transmittance vs. thickness is shown in Figure 1. The transmittance ranges from approximately T=82% for a 2-nm-thick film, to T=2% for a 100-nm-thick film. We have fit the transmittance data using IMD to determine the values of n and k (the real and imaginary parts of the complex index of refraction) for the a-C films: the best fit values so obtained – (n,k)=(1.916, 0.758) – differ somewhat from the values (n,k)=(1.730,0.712) given by Palik [5]. Using the best-fit optical constants, we note that a 200-nm-thick film would have a transmittance of T=0.065%.

To determine the stability of these films, the transmittance was also measured as a function of time. Samples were inserted into the illuminator of an Integrated Solutions DUV exposure tool and irradiated with light at the exposure wavelength (248nm). The power at the wafer plane during exposure was ~140 mW/cm^2 (as measured with the 10-nm-thick sample inserted in the beam.) The resultant plot of transmittance-vs.-time is shown in Figure 2 for two samples; there is no measurable change in transmittance after 80 minutes of exposure. This would correspond to approximately 450 device wafers assuming 50 die/wafer at a dose of 30 mJ/die, and thus suggests that these films are well-suited for long-term use as optical elements in device fabrication.

3. Masked-Deposition Technique For VTA Fabrication

The VTA's used to obtain the results described in reference [1] consist of a concentric ring pattern of a-C films of various thickness, deposited onto a 150 mm-diameter x 0.5-mm-thickness quartz substrate, as shown schematically in Figure 3(a). The film thickness in each of the four rings indicated in Fig. 3(a) was adjusted (by varying the rotational velocity of the substrate over the source as described in Section 2) in order to achieve the desired transmittance values shown in the figure. So, for example, the thickness of the a-C film comprising the outer ring was set to 20 nm, in order to achieve 40% transmittance, and so on for the films used in the other rings. Each film was grown separately, using stencil masks to expose only the relevant portion of the aperture during each deposition cycle. A photograph of the VTA, mounted in the holder needed for installation in an Integrated Solutions Model 8800 Deep Ultraviolet step and repeat exposure tool, is shown in Fig. 3(b). Also shown in Fig. 3(b) are the stencil masks used to produce the VTA.

The masked-deposition technique to control the two-dimensional film thickness profile just described can be used to produce many different types of VTA patterns, and is not limited to the concentric-ring-type pattern as shown in Fig. 3(a). For example, we have recently developed 'dipole', 'tripole', and 'quadrapole' VTA's, which are shown in Figs. 3(c-e). By varying the pole position in this type of VTA, we are able to optimize the illumination (thus increasing the process latitude) for specific feature geometries: for example, the dipole VTA is well suited for a continuous grating geometry, while the tripole could be used for a hexagonal array geometry; the quadrapole VTA could be used to optimize process latitude in so-called Manhattan geometries. We will describe elsewhere specific improvements in process latitude obtained with the VTA's shown in Figs. 3(c-e).

4. Conclusions

We have described the fabrication by magnetron sputtering of amorphous carbon films, and have shown how the DUV optical properties of these films were measured. Because of their desirable optical properties and their excellent stability to high-intensity DUV radiation, these films are well-suited for use as optical elements in high-throughput DUV steppers for sub-0.25-micron lithography. We have used these films to produce variable-transmission apertures that are designed to improve process latitude in DUV lithography, and have described a masked-deposition technique used to fabricate such apertures. Finally, we note that these films are also ideally suited for use in attenuated phase-shift masks for DUV lithography [6]: using the optical constants determined from the measured transmittance, as described in Section 2, we calculate that a ~75-nm-thick a-C film should have a transmittance of ~6% at λ=248 nm and should give rise to a phase-shift on transmission of 180°. Similarly, we estimate (using the optical constants from reference [5]) that a ~58-nm-thick film should also have a phase-shift of 180° and a transmittance of ~8% at λ=193 nm. Therefore, these films can also be used for attenuated phase-shift masks at λ=193 nm.

5. Acknowledgements

We would like to thank G.R. Weber and E.J. Ferry for their help in completing this project.

Figure Captions

Figure 1.. Measured transmittance (diamonds) of a-C films deposited onto quartz substrates, at a photon wavelength of λ=248 nm. The calculated transmittance (dotted line) is also shown, computed from the best-fit values of the optical constants (n,k) as indicated.

Figure 2.. Measured transmittance for two a-C films as a function of time after exposure to high-intensity 248-nm radiation, as described in the text.

Figure 3. Schematic diagram (a) of a concentric-ring-type variable transmission aperture. A photograph of the actual aperture is shown in (b), along with the stencil masks used during fabrication, as described in the text. Dipole (c), tripole (d), and quadrapole (d) apertures are also shown, along with the stencil masks used for fabrication.

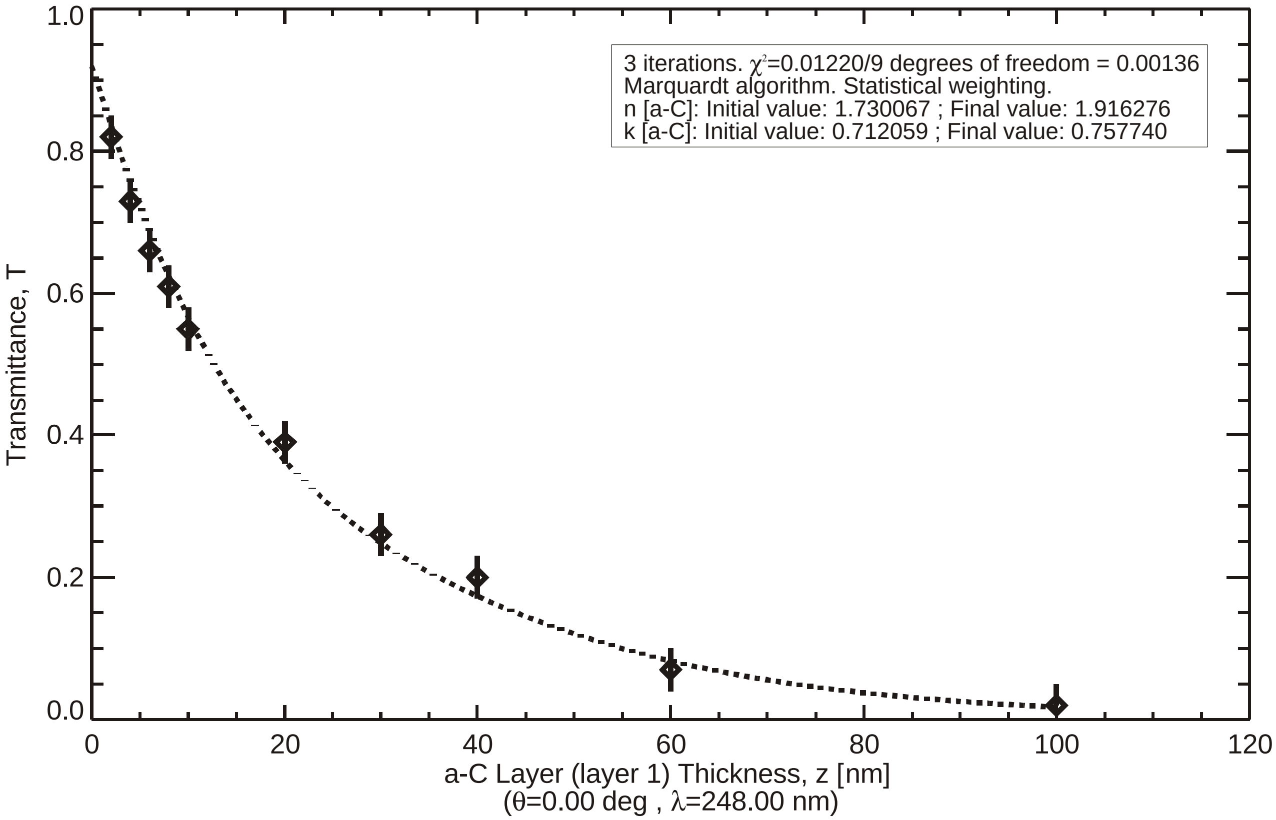
3 iterations. χ²=0.01220/9 degrees of freedom = 0.00136
Marquardt algorithm. Statistical weighting.
n [a-C]: Initial value: 1.730067 ; Final value: 1.916276
k [a-C]: Initial value: 0.712059 ; Final value: 0.757740
Transmittance, T
1.0
0.8
0.6
0.4
0.2
0.0
0
20
40
60
80
100
120
a-C Layer (layer 1) Thickness, z [nm]
(θ=0.00 deg , λ=248.00 nm)

Figure 1.

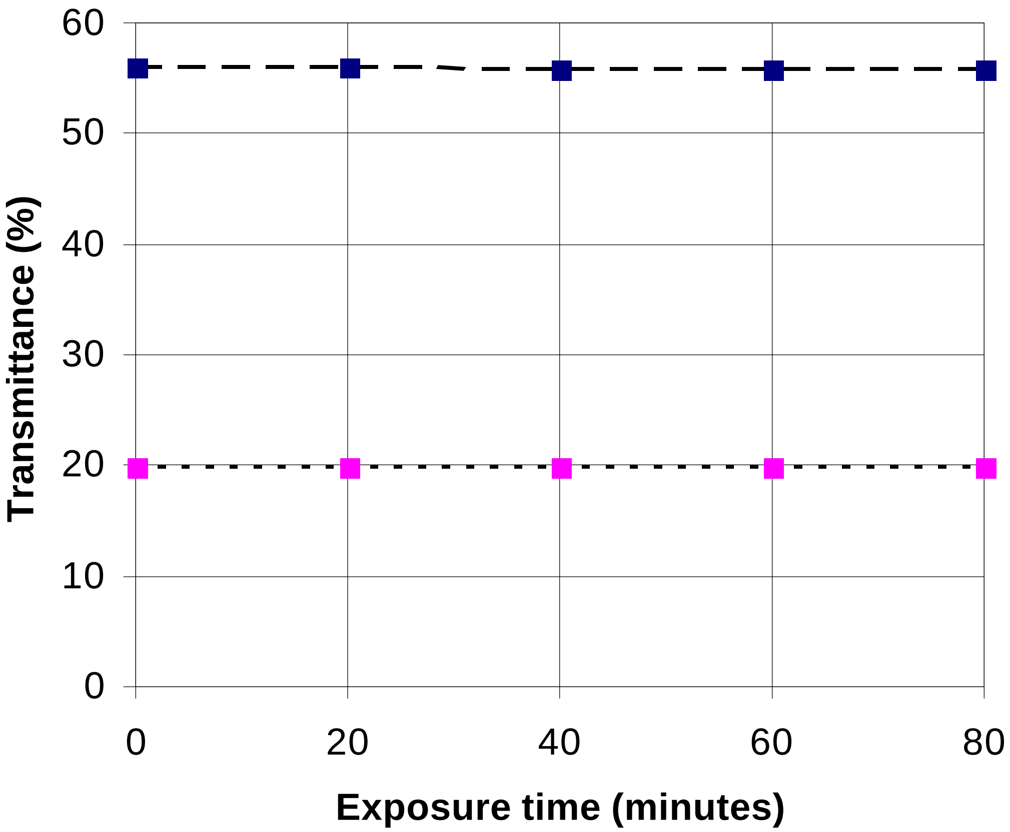

60
50
40
30
20
10
0
Transmittance (%)
0
20
40
60
80
Exposure time (minutes)

Figure 2.

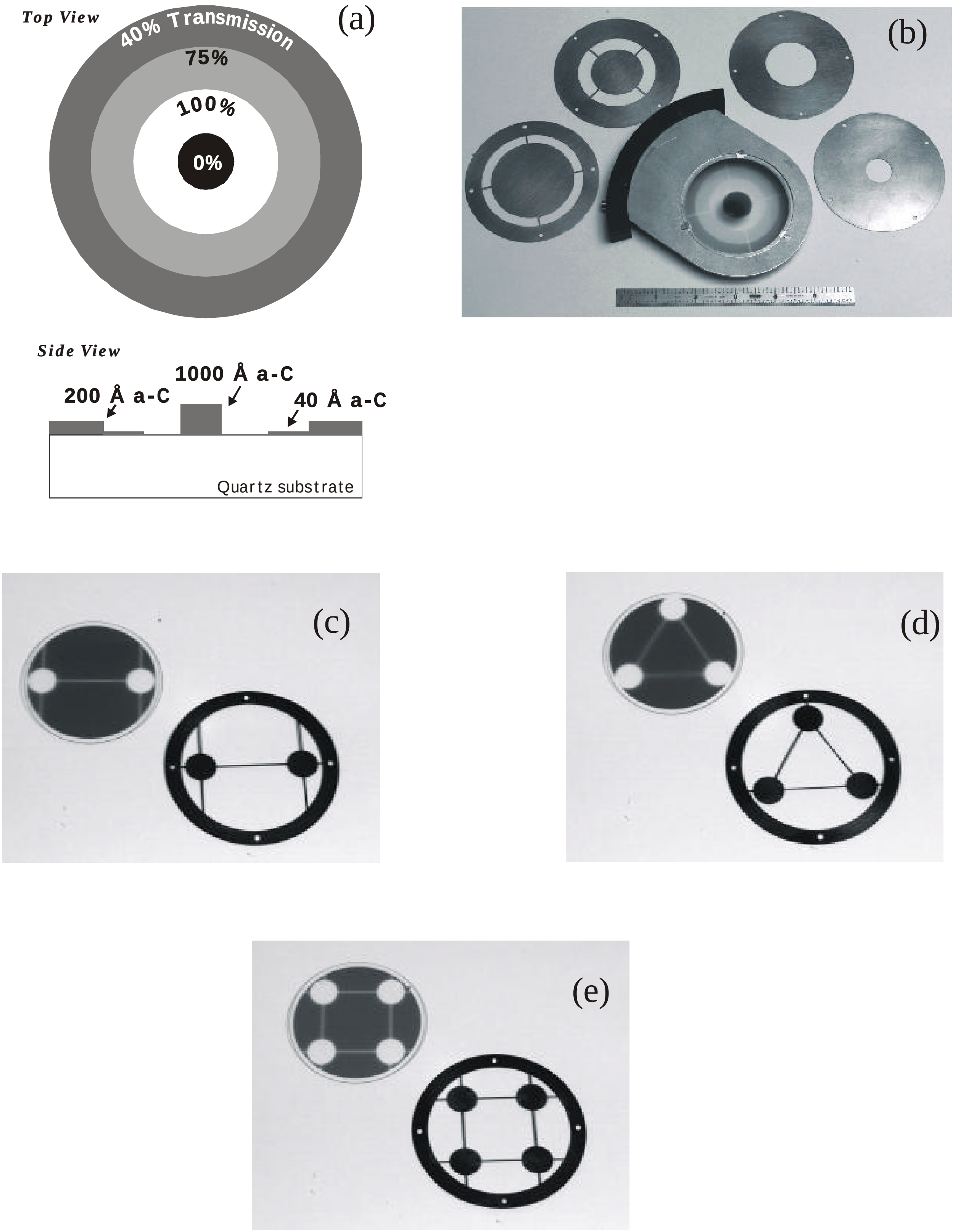
Top View
40% Transmission
75%
100%
0%
(a)
Side View
1000 Å a-C
200 Å a-C
40 Å a-C
Quartz substrate
(b)
(c)
(d)
(e)

Figure 3.

References

1. R. A. Cirelli, M. Mkrtchyn, G. P. Watson, L. E. Trimble, G. R. Weber, D. L. Windt, and O. Nalamasu, *Proc. SPIE*, **3334,** 395-405 (1998)

2. D. L. Windt and W. K. Waskiewicz, *J. Vac. Sci. Technol. B*, **12**, 3826-3832 (1994)

3. D. L. Windt, *Computers in Physics*, **12**, 360-370 (1998)

4. D. G. Stearns, *J. Appl. Phys*. **65**, 491-506 (1989)

5. ‘Handbook of Optical Constants of Solids’, edited by E. Palik, Academic Press, Inc., Orlando, FL, 1986

6. Y.C. Ku, Erik H. Anderson, Mark L. Schattenburg, Henry I. Smith J. Vac. Sci. Technol, B, **6** 150-154 (1987)